OPTIMAL OBSERVATIONAL CONDITIONS OF THE PLANETARY SURFACE FOR THE RELIEF RECONSTRUCTION WITH PHOTOMETRIC METHOD. ***S. I. Skuratovsky, I. A. Dulova, Yu. V. Kornienko, N. V. Bondarenko*** , Institute of Radiophysics and Electronics, National Academy of Science of the Ukraine, 12 Ak. Proskury, Kharkov, 61085, Ukraine.

Introduction. High-resolution topographic information is important in different applications for the study of planetary surfaces: their evolution, state, and properties.

The most precise topographic data are obtained through direct measurements with different altimeters on board of spacecrafts (e.g., [1]). Indirect techniques for surface height estimates involve photogrammetry (e.g., [2]), photoclinometry (e.g., [3]), and interferometry (e.g., [4]).

Illumination-viewing conditions for observations of planetary surface are important for relief reconstruction with indirect methods. These conditions are usually limited during real missions by spacecraft orbit geometry, particular time of observations, spacecraft life time and scientific program which lead to the limited number of observations of the same surface areas.

In the present work we analysis relationship between illumination-viewing conditions of surface observations and spatial error distribution arose during surface relief reconstruction with photometric method proposed in [5]. The method is the most mathematically correct and can be classified as a photoclinometry method since it uses the fact that observed brightness of the surface depends on the surface orientation.

The study was made using simulated observations of the test surface in the optical wavelength range and for radar experiments.

Photometric method for the planet relief determination. The photometric method used here is based on the statistical approach to a problem of surface relief determination from a set of images taken under different viewing conditions. The brightness (J) of an element with coordinates (x, y) in the j-th image can be written as

$$J_j(x,y) = \int_{-\infty}^{\infty}\int_{-\infty}^{\infty} g_j(x-x', y-y') I_j(x',y')dx'dy' + N_j(x,y). \quad (1)$$

N_j(x,y) is a realization of recording noise, $g_j(\cdot)$ describes the blurring of the true brightness distribution $I_j(x,y)$ due to recording system transfer function, phase distortions of the radiation during the propagation through a medium, and so on.

For small surface tilts, the true surface brightness $I_j(x,y)$ can be expanded into a Taylor series, and with two series terms it can be presented as

$$I_j(x,y) = I_{0j} + c_{xj}\frac{\partial H(x,y)}{\partial x} + c_{yj}\frac{\partial H(x,y)}{\partial y}, \quad (2)$$

where the pair ($\partial H/\partial x$, $\partial H/\partial y$) is a two-dimensional height gradient vector, and the pair (c_{xj}, c_{yj}) is the first derivative of the photometric function. In the frame of our approach, the photometric function has to be known a priori.

For an ideal case with no noise, the set of equations (1) and (2) gives exact solution for the surface relief $H(x,y)$ (the height deviation above a mean plane). For actual experimental data accompanied by the noise, the same set may allow no solution at all. So, the problem of relief determination from a set of images in the presence of noise is improper posed. The best way to solve the problem with real observations is the statistical approach. This approach allows determination of the height distribution that is the most probable for the given set of images (Eq. 1).

The true relief $H(x,y)$ of the surface under study and the noise N_j(x,y) are considered to be a realization of stationary Gaussian random process.

The relief determination from the set of images and image processing are fulfilled in the spatial frequency domain (frequency coordinates are denoted as k_x,k_y). The expression for the most probable relief $H_M(k_x,k_y)$ can be deduced through following steps. At first, a posteriori probability density of the relief is derived with the Bayes' formula [6]. Then it is converted into the log-likelihood function that is the logarithm of the posteriori relief probability density. The first derivative of the log-likelihood function equated to zero (condition for the maximum) gives an equation for the most probable relief. The solution of this equation leads to the following expression for the most probable relief $H_M(k_x,k_y)$:

$$\tilde{H}_M(k_x,k_y) = \frac{i\sum_j D_j \tilde{g}_j^*(k_x,k_y)\beta_j(k_x,k_y)\tilde{J}_j(k_x,k_y)}{\alpha(k_x,k_y) + \sum_j (D_j)^2 W_j}, \quad (3)$$

where $W_j = \tilde{g}_j^*(k_x,k_y)\tilde{g}_j(k_x,k_y)\beta_j(k_x,k_y)$, and $D_j = k_x c_{xj} + k_y c_{yj}$. Here $\tilde{g}_j(k_x,k_y)$ and $\tilde{J}_j(k_x,k_y)$ are Fourier transforms of $g_j(x,y)$ and $J_j(x,y)$, respectively; " * " means complex conjugation. $\alpha(k_x,k_y)$ and $\beta_j(k_x,k_y)$ are reciprocal of height and noise spectral density, respectively.

Eq. (3) specifies an optimum filter for derivation of the most probable relief from the set of images. This filter depends strongly on a-priori known factors that distort received signals. This approach can correctly account for statistically independent additive gaussian noise and blurring factor.

Viewing conditions and error fields for the determinated relief. For the present study we used test

lunar-like cratered surface. Slopes of the test surface shown in Fig. 1 are varied between 0 and 31° as for real planetary surfaces. The highest slopes are located at the largest crater rim (brightest shadows in Fig. 1).

We obtained sets of images of the test surface with two photometric functions to simulate optical and radar observations. Lambert law was chosen as a photometric function described light scattering in the optical wavelength range, and Muhleman law [7] specified for radar observation of the Venus surface [8] was used to simulate radar experiment. Examples of initial optical and radar images used for the relief reconstruction are shown in Fig. 2a and Fig. 3a, respectively. We chose the geometry of experiments when direction to the source of the flux is coincided with direction to the receiver as for radar experiments. Incidence angle was 35.5°. In Fig. 2a, 3a the direction of surface illumination is shown with arrows. Illumination-viewing azimuth angle (*A*) here is 90° (anticlockwise from the bottom). Images in Fig. 2a, 3a are differed rather high from each other in brightness contrast. Brightness contrast is higher for radar observations (Fig. 3a).

We reconstructed surface topography with Eq. 3 using one image and two images with different illumination-viewing azimuths. Spatial distributions of differences between calculated and test relief are shown in Fig. 2, 3 for: (b) – one initial image (*A*=90°); (c) – two initial images (*A*=90°, -90°); (d) – two initial images (*A*=0, 90°). Spatial distributions of height errors are similar when relief was reconstructed using one image (Fig. 2b) and two images observed from opposite to each other sides (Fig. 2c) for simulated optical observations. These distributions depend strongly on image coordinate that is normal to the viewing direction. For radar experiments such distributions are different (Fig. 3b, 3c). Absolute errors of heights estimates were lower with the use of two initial images.

Errors distributions of heights reconstructed using two images obtained at normal to each other illumination-viewing directions depend on both coordinates (Fig. 2d, 3d). Errors values in this case are the lowest.

Conclusion. Thus, model calculations confirmed that images obtained at normal to each other illumination (viewing) directions are the most preferable for relief reconstruction. The most unfavorable for such purposes is the use of images obtained from opposite to each other directions.

Calculation also shows that relief cannot be reliable reconstructed using one image. But for some cases the use of one image is enough for identification of relief shapes.

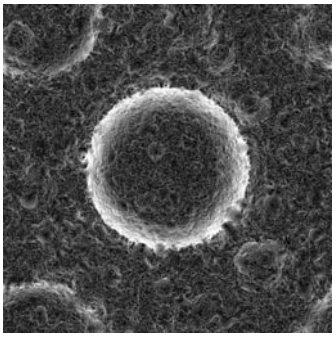

Fig. 1.

References: [1] . Smith, D. E. et al (2001) *J. Geophys. Res.* **106**, E10, 23,689. [2] Herrick, R. R.; Sharpton, V. L. (2000) *J. Geophys. Res.* **105**, E8, 20,245. [3] Wildey, R. L. (1990) *Earth, Moon, and Planets* **48**, 197-231. [4] Margot, J.-L. et al. (1999) *J. Geophys. Res.* **104**, E5, 11,875 [5] Kornienko Yu.A., Dulova I.A., Nguyen Xuan Anh. (1994) *Kinematics and Physics of Stellar Bodies* **10**, 69 – 76. [6] Love M. *The probability theory* (1962). [7] Muhleman D.O. (1964) *Astron. J.* **69**, 34 – 41. [8] Ford P.G. and Pettengill G.H. (1992) *JGR Planets* **97**, 13,103 – 13,114

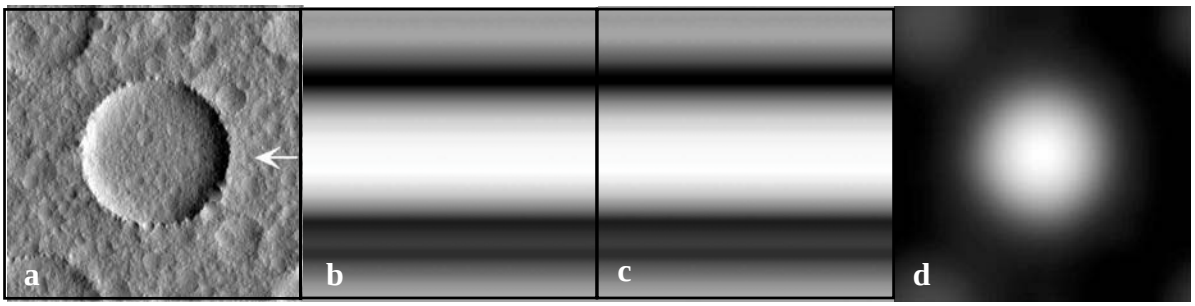

Fig. 2

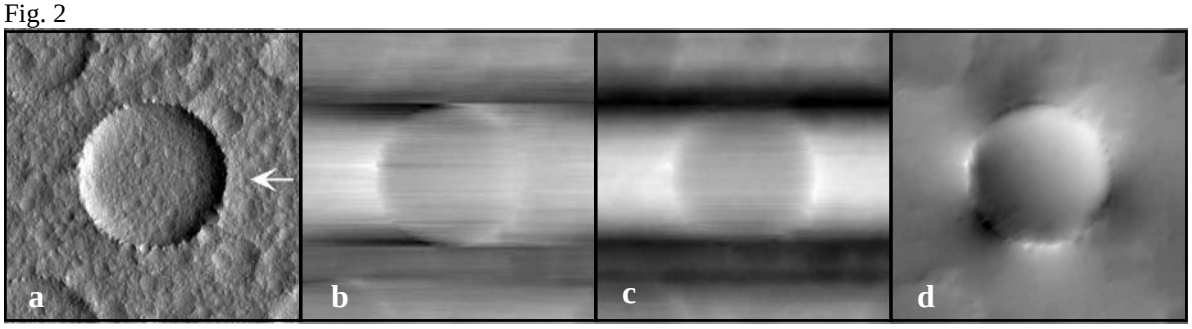

Fig. 3